Journal of Zhejiang University-SCIENCE B (Biomedicine & Biotechnology) *in press*
www.jzus.zju.edu.cn; www.springer.com/journal/11585
E-mail: jzus_b@zju.edu.cn

Research Article

https://doi.org/10.1631/jzus.B2400427

An integrative combination of gas-liquid-phase plasma mutagenesis and high-throughput screening to enhance eicosapentaenoic acid production by *Schizochytrium* sp.

ChaoYU[1,2,3*], Jialin ZHU[4,5,6*], Jinyong WU[2], Xiangsong CHEN[1,2], Shuhuan LU[3], Xiangyu LI[3], Sa ZHAO[3], Weiwei ZHU[3], Min SHU[3], Mianbin WU[4,5,6✉], Jianming YAO[1,2✉]

[1]*University of Science and Technology of China, Hefei 230026, China*
[2]*Hefei Institutes of Physical Science, Chinese Academy of Sciences, Hefei 230031, China*
[3]*Cabio Biotech (Wuhan) Biotechnology Co. Ltd., Wuhan 430223, China*
[4]*Key Laboratory of Biomass Chemical Engineering of Ministry of Education, College of Chemical and Biological Engineering, Zhejiang University, Hangzhou 310030, China*
[5]*Ningbo Research Institute, Zhejiang University, Ningbo 315100, China*
[6]*Zhejiang Key Laboratory of Antifungal Drugs, Taizhou 318000, China*

Abstract: Dietary consumption of eicosapentaenoic acid (EPA) offers diverse health benefits like regulation of blood triglycerides and prevention of cardiovascular diseases. EPA is naturally synthesized by *Schizochytrium* sp.; however, its low production level limit its potential for industrial application. The goal of this study was to increase EPA productivity in *Schizochytrium* sp. by gas-liquid-phase plasma mutagenesis (GLPP) combined with a high-throughput screening method. First, a diverse array of mutants was generated through GLPP mutagenesis. Next, the mutants with elevated EPA productivity were identified through near-infrared spectroscopy. Notably, the M7-25 mutant demonstrated the highest and most consistent EPA production. After the culture medium was optimized, the EPA titer increased from 0.45 to 1.70 g/L. Finally, a cofermentation strategy using ammonia and glucose feeding was employed, and the EPA titer reached 2.08 g/L in a 7 L fermenter. To date, this is the highest EPA titer reported in *Schizochytrium* sp. using mutagenesis technology, indicating its great market potential for industrial production.

Key words: Eicosapentaenoic acid (EPA); *Schizochytrium* sp.; Mutagenesis; High-throughput screening; Near-infrared spectroscopy

✉ Jianming YAO, jmy63@ipp.ac.cn
Mianbin WU, wumb@zju.edu.cn
* The two authors contributed equllay to this work
Jianming YAO, https://orcid.org/0000-0001-6469-5380
Mianbin WU, https://orcid.org/0000-0001-6962-9702
Chao YU, https://orcid.org/0009-0002-6291-699X
Jialin ZHU, https://orcid.org/0009-0000-3313-2315

Received Aug. 19, 2024; Revision accepted Oct. 13, 2024;
Crosschecked xxx. xx, 20xx; Published online xxx. xx, 20xx

1 Introduction

Eicosapentaenoic acid (EPA) is an important functional food component that strongly supports human growth and development (Jia et al., 2022). Numerous studies have confirmed the effectiveness of EPA in preventing cardiovascular disease (Bhatt et al., 2019; Preston Mason, 2019; Khan et al., 2021), cancer (Liu et al., 2021b; Yin et al., 2022), and depression(Bazinet et al., 2020; Peng et al., 2020); reducing inflammation (Calder, 2013; Lamon-Fava et al., 2021); and improving cellular antioxidant capacity(Xiao et al., 2022). Furthermore, recent research has shown that EPA may significantly reduce coronavirus disease symptoms (Doaei et al., 2021; Kosmopoulos et al., 2021). The demand for EPA has been growing at a rapid pace. EPA is mainly found in oily deep-sea fish such as salmon, tuna and mackerel. However, the current supply of EPA from aquaculture and fisheries meets only 30% of the global demand (Hamilton et al., 2020) due to factors such as increasing global population and stagnation of fishery production over the past five years caused by global warming (Auchterlonie and Bescoby, 2021). Thus, methods to sustainably manufacture EPA are desperately needed to eliminate shortages.

To address the current shortage, researchers are searching for alternative sources of EPA, particularly from microorganisms. *Schizochytrium* sp. is considered an excellent candidate for EPA production because of its naturally high lipid content and its EPA synthesis pathway. *Schizochytrium* sp., belonging to the *Thraustochytrids* family, is a heterotrophic marine microalgal commonly found in seawater in Australia (Gupta et al., 2013), China (Ling et al., 2015), the Antarctic region (Shene et al., 2020), and other areas. Since the 1990s, *Schizochytrium* sp. has been utilized for commercial production of docosahexaenoic acid (DHA) (Ratledge and Hopkins, 2006). However, compared to production of DHA, production of EPA by *Thraustochytrids* strains is much less efficient. Jiang et al. isolated five *Thraustochytrids* strains and found that the ratio of EPA to total fatty acid (TFA) was no more than 1% (Jiang et al., 2004). A strain isolated by Shene et al., Antarctic *Thraustochytrids* RT2316-7, exhibited an EPA/TFA ratio of 16.4% when cultured at 15 ℃ (Shene, et al., 2020). However, the overall lipid content of this strain was extremely low.

To improve EPA productivity, Zeng et al applied atmospheric and room-temperature plasma (ARTP) mutagenesis to *Schizochytrium* ATCC 20888, producing a mutant with an EPA titer of 0.48 g/L which was 1.08-fold greater than that of the wild-type strain (Zeng et al., 2021). Ou et al also applied ARTP mutagenesis to *Schizochytrium* ATCC 20888, achieving an EPA titer of 1.86 g/L, with EPA accounting for 5.86% of the TFA (Ou et al., 2023). Although the EPA productivity of *Schizochytrium* has improved, industrial application is still a distant possibility due to its low productivity and EPA content. The use of mutagenesis to improve EPA productivity in *Schizochytrium* has several technical limitations. The primary challenge involves generation of mutants with highly diverse fatty-acid profiles. Efficiently identifying mutants with high EPA productivity from a large pool of candidates is another obstacle. In response to these challenges, we employed a new physical mutagenesis technique known as gas-liquid-phase plasma (GLPP) mutagenesis. As depicted in Fig. 1, GLPP is generated from the discharge of O_2/air gas into the cell cultivation broth, which results in the generation of reactive nitrogen species ($NO/HNO_2/HNO_3/ONOOH$) and reactive oxygen species ($OH/H_2O_2/O_3$) in the liquid phase (Morabit et al., 2021). These reactive species can inflict damage on cellular structures or genomes, potentially causing mutations or cell death. Consequently, GLPP is commonly employed to sterilize water contaminated with bacteria (Shen et al., 2019). However, by carefully modulating the discharge energy, GLPP can be employed to induce mutations in microorganisms. Regarding the second challenge, gas chromatography (GC), a traditional method for determining FA composition, is labor-intensive and time-consuming. In contrast, recent advances in near-infrared spectroscopy (NIRS) offer a swift and nondestructive alternative for determining the chemical composition of a compound or solution; this technique works by measuring the absorption of near-infrared radiation; indeed, several studies have demonstrated that NIRS can be utilized to assess FA compositions (Yu et al., 2020; Reis et al., 2022; Tsegay et al., 2023).Because of the advantages of GLPP and NIRS, we combined these two powerful tools to establish a highly efficient platform for generating and detecting mutants with different levels of EPA productivity, as presented in Fig. 1.

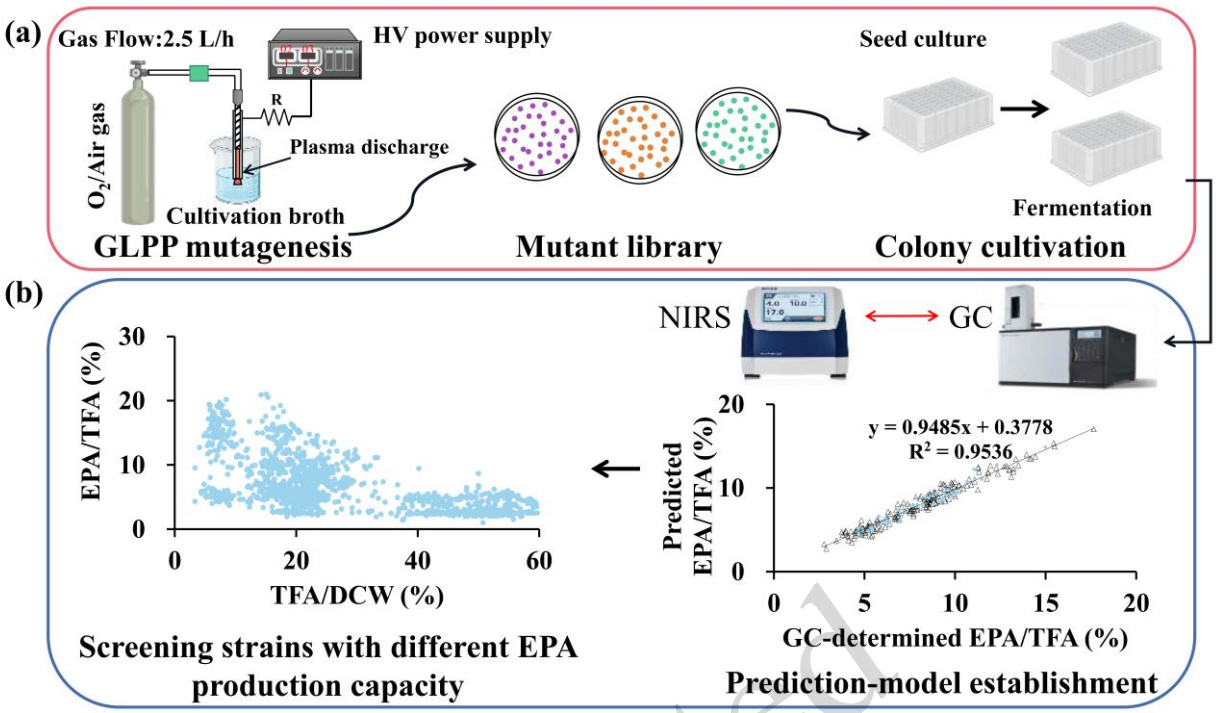

Fig. 1 Design of the gas-liquid-phase plasma (GLPP) mutagenesis and high-throughput screening platform for generating strains with different eicosapentaenoic acid (EPA) production capacities. (a) Liquid culture of *Schizochytrium* sp. was treated with GLPP to generate a mutant library. Single colonies were cultured in 24-well plates as seed-cultivation broth and then transferred to different 24-well plates for fermentation. (b) Samples of fermentation broth were scanned with near-infrared spectroscopy (NIRS) and analyzed with gas chromatography (GC), which generated enough data to establish a robust NIRS prediction model. This model was subsequently used to predict the EPA-production ability of the mutant strains.

In this study, we aimed to improve the production of EPA by *Schizochytrium* sp. through mutagenesis. First, we used GLPP to create a broad array of mutants in *Schizochytrium* sp. Then we developed an analytical method using NIRS technology to measure the ratio of TFA to dry cell weight (DCW) and determine the FA composition of the mutants. Genetic stability assessment was performed to confirm that the M7-25 mutant was stable for EPA production. Next, we optimized the concentrations of salt and phosphorus to increase the EPA titer. This step increased the concentration of TFA from 8.38 g/L to 18.64 g/L and increased the EPA titer substantially from 1.15 g/L to 1.58 g/L. Furthermore, when fermentation was scaled up to 7 L, the EPA titer of M7-25 reached 2.08 g/L, and the EPA/TFA ratio increased to 9.58%, representing a 1.77-fold and 3.05-fold increase, respectively, compared with the titer and ratio in the WT strain. We obtained a large number of mutant strains by GLPP mutagenesis, and then used high-throughput NIRS technology to identify mutant strains with high EPA production (Fig. 1). After performing medium and process optimization, we achieved the highest level of EPA production among known nongenetically manipulated *Schizochytrium* sp. strains, demonstrating that strain has significant potential for large-scale industrial production.

2 Materials and methods

2.1 Strain, medium and cultivation conditions

Schizochytrium sp. A-2 (CCTCC No: M2012494) was used as the starting strain. The seed culture medium consisted of glucose (50 g/L), sodium glutamate (20 g/L), yeast extract (10 g/L), KH_2PO_4 (3 g/L), $MgSO_4$ (8 g/L), and NaCl (20 g/L). The fermentation medium consisted of glucose (100 g/L), sodium glutamate (20 g/L), yeast extract (15 g/L), and KH_2PO_4 (1.5 g/L) supplemented with either artificial sea salt or natural sea salt (NSS, East Sea of China). The artificial sea salt included $MgSO_4$ (3 g/L), Na_2SO_4 (25 g/L), $(NH_4)_2SO_4$ (5 g/L), KCl (1 g/L), $CaCl_2$ (0.15 g/L), and $NaHCO_3$ (0.2 g/L).

For high-throughput cultivation, the mutants were inoculated into 48-deep-well plates, with each well containing 1.5 mL of the seed culture medium. The plates were placed in a shaker at 28 °C with shaking at 230 r/min for 36 h. At the end of cultivation, the seed broth was transferred to another 48-deep-well plate, with each well containing 1.5 mL of fermentation medium. These plates were incubated again under the same conditions for 120 h.

For shake-flask fermentation, the mutants were cultured in seed culture medium for two generations, after which 2 mL of the seed medium was transferred to 250 mL shake flasks that were filled with 40 mL of fermentation medium. The fermentation experiments were carried out in a shaker set at 28 °C for 120 h with shaking at 230 r/min. The pH of the medium was not adjusted.

2.2 GLPP Mutagenesis

The starting strain was cultivated in a 250 mL shake flask. Following incubation, the culture broth was centrifuged at 6000 r/min for 5 min, after which the cells were harvested and washed with 20 mL of sterile water. The washed cells were resuspended in sterile 9 g/L NaCl solution, with the volume matching the original culture volume, resulting in an optical density (OD_{600}) of approximately 20. The cell suspension was treated with GLPP for 5, 10, 15 or 20 minutes. The discharge power of the GLPP was set at 12.7 V, and the discharge peak current was set at either 1.5 or 2 A. Subsequently, the sample was diluted, spread on solid plates, and incubated at 28 °C for 48 h. The number of colonies was recorded, and the lethality of the cells was calculated according to the following formula:

$$\text{Lethality (\%)}=\frac{\text{Colonies counts of control - Colonies counts with GLPP}}{\text{Colonies counts of control}}\times 100.$$

2.3 Quantification of dry cell weight and total fatty acid, and fatty-acid composition

Dry cell weight (DCW) was quantified as follows: 1.0 mL of fermentation broth was harvested, and the cells were collected by centrifugation (6000g, 3 min), followed by lyophilization. The DCW was calculated as follows: DCW (g/L) =freeze-dried cell weight (mg)/sample volume (mL).

For TFA extraction and fatty acid methyl ester (FAME) analyses, we followed the method described by Yue et al (Yue et al., 2019). The EPA/DCW was calculated by the internal standard method (Golay and Moulin, 2016). The EPA/TFA ratio was the proportion of the peak area of EPA to the total peak area. The TFA/DCW ratio was calculated using the following formula:

$$\text{TFA/DCW}=\frac{\text{EPA/DCW}}{\text{EPA/TFA}}$$

2.4 Prediction-model development by NIRS

The FOSS NIR spectrophotometer uses diffuse reflection to measure the transmission and reflectance spectra of a sample over a wavelength range of 570 to 1880 nm. A total of 2 mL culture broth was centrifuged at 6000 r/min for 5 min, after which the cells were harvested and washed with 10 mL of tap water. The washed cells were then dispersed in 2 mL tap water. The cell suspension was scanned five times to form an average NIR spectrum, which was then transformed into log (1/R) format. We developed prediction models to quantify the

TFA/DCW as well as the proportion of palmitic acid (PA), arachidonic acid (ARA), EPA, docosapentaenoic acid (DPA) , and docosahexaenoic acid (DHA) to TFA .We used the modified partial least squares regression method, and implemented it in WinISI III software (InfraSoft International, LLC, FOSS). The data-quality assessment was evaluated using the root mean square error of cross-validation for each individual dataset.

2.5 Evaluation of mutants' genetic stability

The candidate mutants were cultivated in seed medium for seven successive passages. Each cultivation of the passage represented one generation, and the cultivation of each passage was inoculated into the fermentation medium and cultivated for 5 days. Then, the ratios of EPA/TFA and TFA/DCW were measured and compared with the ratios from the first generation. The mutant with the most stable genetic performance was used for further experiments.

2.6 Medium optimization and fed-batch fermentation

2.6.1 Shake-flask fermentation to optimize the medium

We used biological triplicates to analyze the DCW, FA composition and TFA/DCW ratio. The medium optimization was performed as follows: (1) Salinity experiments: artificial sea salt and NSS were both tested at concentrations of 15, 25, 35, and 45 g/L, and the other components of the medium included 100 g/L glucose, 20 g/L sodium glutamate, 7.5 g/L yeast extract and 1.5 g/L KH_2PO_4. (2) Phosphorus experiment: KH_2PO_4 concentrations were tested at concentrations of 0.1, 0.5, 1.5, and 3.5 g/L, and the other components of the medium were 25 g/L NSS, 100 g/L glucose, 20 g/L sodium glutamate, and 7.5 g/L yeast extract.

2.6.2 Fed-batch fermentation in a 7-L fermenter

The fed-batch fermentation was conducted using 7-L fermenters (Shanghai Baotech Engineering Co.,Ltd, China). Three different fermentation batches were performed using: (1) WT strain, (2) M7-25 mutant strain, and (3) M7-25 mutant strain which was fed 25% $NH_3 \cdot H_2O$ for 10-48 h. The seed culture was transferred to 4 L of fermentation medium with an inoculation ratio of 5% (volume fraction). The fermentation medium components were 25 g/L NSS, 100 g/L glucose, 20 g/L sodium glutamate, 7.5 g/L yeast extract, and 0.5 g/L KH_2PO_4. The fermentation temperature was set at 28 ℃, and the pH was maintained at 7.6 by adding citrate acid. The dissolved oxygen was maintained at no lower than 20% for 0-48 h and no higher than 10% for 48-144 h by adjusting the air-flow rate and agitation speed. The residual glucose concentration in the fermentation broth was maintained between 10-30 g/L by feeding a 600-g/L glucose solution. Fermentation broth was sampled every 12 h to analyze the DCW, TFA/DCW, and FAs/TFA. In addition, we performed pH experiments under the same fermentation conditions, in which the pH was maintained at 7.6 using various acid-base combinations: (1) citric acid + ammonia solution, (2) citric acid + sodium hydroxide, and (3) ammonium sulfate + sodium hydroxide.

2.7 Statistical analysis

The results are presented as the mean ± standard deviations. Statistical significance between mean values was determined using Duncan's test.

3 Results and discussion

3.1 GLPP mutagenesis of *Schizochytrium* sp.

Schizochytrium sp. is the most commonly used strain for commercial production of DHA. It also has the ability to synthesize small amounts of EPA (Gupta, et al., 2013; Shene, et al., 2020). In this study, we employed the GLPP mutagenesis method to produce mutant strains of *Schizochytrium* sp. and obtain strains with high EPA

productivity for industrial application.

As shown in Fig. 2a, the lethality rate of cells increased rapidly at 5 min of exposure to GLPP at two different discharge peak currents. When the exposure time was increased, the lethality rate decreased, which was consistent with the results of ARTP mutagenesis (Wei et al., 2023). After a 20-minute exposure, the maximal lethality of the cells reached 82.4% and 98.1% at discharge peak currents of 1.5 A and 2.5 A, respectively ($p < 0.05$). These results indicated that compared to a lower current, a higher discharge peak current led to a higher lethality rate. To achieve a lethality rate of 90% (Liu et al., 2021a), we selected the condition of optimal discharge peak current of 2.5 A and an exposure period of 15 minutes to achieve a lethality rate of approximately 93.5%. The fatty-acid composition varied broadly in the resulting mutants compared with the WT strain, with EPA/TFA ranging from −38.44% to 68.5% and ARA/TFA ranging from −41.23% to 46.69% (Fig. 2b); in contrast, the variability for DHA/TFA and DPA/TFA was mainly in the range of -20% to 20% (Fig. 2c). The relative variation in palmitic acid ranged from 39.35% to -72.38% (Fig. 2d). The substantial range in EPA/TFA and ARA/TFA, along with the relative stability in DHA/TFA and DPA/TFA, reflects the high efficacy and randomness of GLPP in inducing relevant mutations. Similar results were reported in recent studies that used ARTP mutagenesis technology in *Schizochytrium*. For example, Wei et al. (Wei, et al., 2023) reported a 108% increase in the EPA titer, Ou et al. (2023) reported a more substantial increase (5.64-fold) in the EPA titer, and Wang et al. (2021) documented a 51% increase in DHA/TFA. These findings showed that ARTP mutagenesis can effectively enhance the biosynthesis of omega-3 fatty acids. In contrast, our study with GLPP mutagenesis revealed a unique trend in which EPA/TFA and ARA/TFA varied substantially, which also showed that GLPP mutagenesis with a discharge peak current of 2.5 A and an exposure period of 15 minutes was effective in inducing mutations that can lead to improved EPA production in *Schizochytrium* sp.

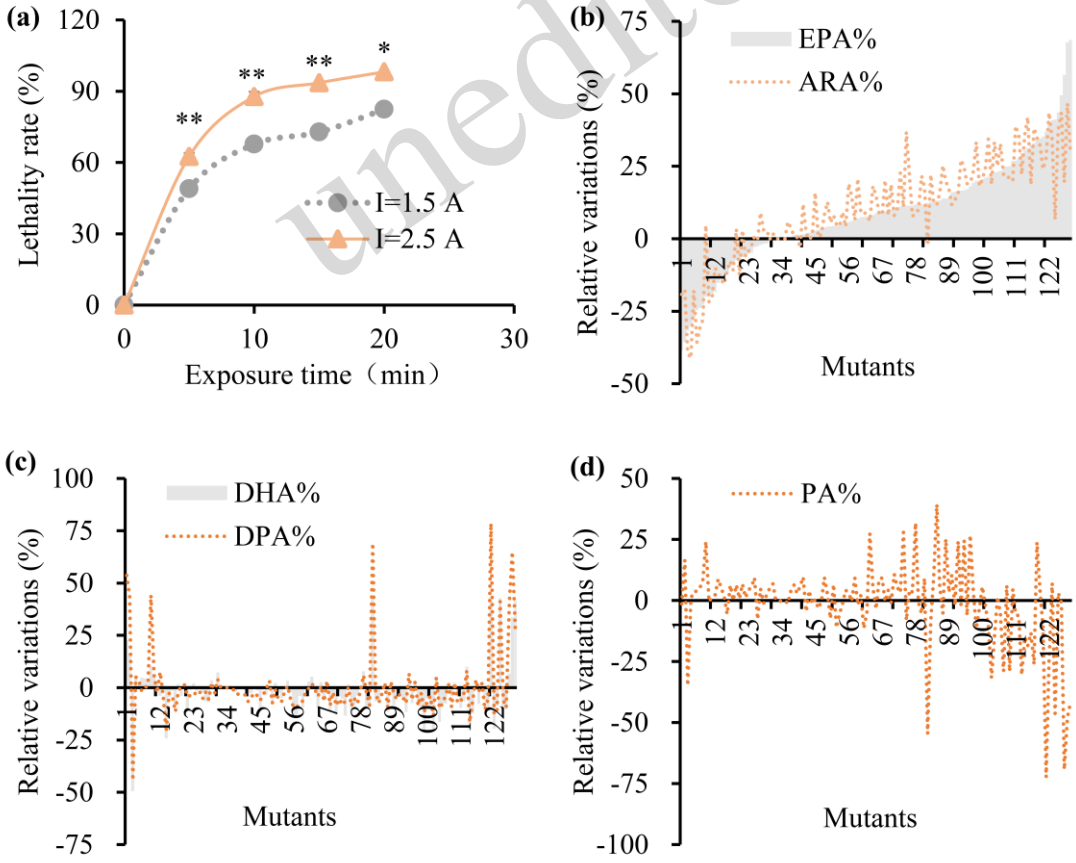

Fig. 2 Effects of gas-liquid-phase plasma (GLPP) on lethality rate and fatty acid composition in *Schizochytrium* sp. mutants.

(a) Effects of different energy levels (*I*=1.5A and *I*=2.5A) and exposure times (5, 10, 15, and 20 min) of GLPP mutagenesis on the lethality rate of *Schizochytrium* sp. The data were collected from three independent experiments. Error bars represent the standard deviation. Significant differences between the *I*=1.5 A and *I*=2.5 A groups are indicated by asterisks (*) (P*<0.05, ***P*<0.01); (b-d)The relative variations in the proportions of eicosapentaenoic acid to total fatty acid (EPA/TFA) and, arachidonic acid to total fatty acid (ARA/TFA) (b), docosahexaenoic acid to total fatty acid (DHA/TFA) and, docosapentaenoic acid to total fatty acid (DPA/TFA) (c), and palmitic acid to total fatty acid (PA/TFA) (d) in the GLPP-induced mutants compared with the WT strain.**

3.2 High-throughput analysis of FA composition by NIRS

Traditional methods for screening mutants can be inefficient and cost-prohibitive (Zeng et al., 2020). Owing to the substantial number of mutants generated by GLPP mutagenesis, we considered it imperative to develop an efficient screening method that could swiftly and accurately identify strains with highly efficient EPA biosynthesis. Here, we used 194 samples for NIRS calibration, employing a modified partial least square regression methodology within WinSIS III to develop prediction models. The NIRS curves displayed a similar trend with abundant absorption in the 1300-1600 nm region, and each sample differed in terms of absorption in this region, which formed the basis for calculating and establishing the NIRS model (Fig. S1).

The key parameters for modeling the FA composition and TFA/DCW ratio are summarized in Table 1. The R^2 values obtained for the TFA/DCW, EPA/TFA, and DHA/TFA calibration modes were 0.963, 0.947 and 0.901, respectively, with the standard error of the cross-validation (SECVs) being 1.555, 0.935, and 1.948, respectively. The results suggest that the NIRS models are satisfactory for predicting TFA/DCW, EPA/TFA, and DHA/TFA, showing the best performance for TFA/DCW. Notably, our R^2 values were greater than those reported by Reis et al. (0.89) (2022) and Yu et al. (0.90) (2020). The improved fit of our model may be due to the removal of impurities from the fermentation broth by washing the cells with tap water, which improved modeling accuracy.

Table 1 Coefficient of determination (R^2) and standard error of cross-validation (SECV) of the calibration set for TFA/DCW and fatty acid/TFA using NIRS

Parameters	R^2	SECV
TFA/DCW	0.963	1.555
EPA/TFA	0.947	0.935
DHA/TFA	0.901	1.948

TFA: Total Fatty Acid, DCW: Dry Cell Weight, DHA: Docosahexaenoic Acid, NIRS: Near-Infrared Spectroscopy

While the high R^2 value indicates that our model fit the training data well, it was also crucial to evaluate its predictive accuracy. To assess the model's accuracy, we selected a set of 48 mutant samples for use as an external validation set. A comparison of the NIRS predictions and reference values for TFA/DCW, EPA/TFA, and DHA/TFA is shown in Fig. 3. The biases between the prediction and reference values for TFA/DCW (Fig. 3a) and EPA/TFA (Fig. 3b) were generally less than 10%; only approximately 8.3% of the samples showed a bias exceeding 10% for EPA/TFA, and none of these biases surpassed 15%. Both the prediction and reference data biases were under 10% for DHA/TFA (Fig. 3c). Notably, the samples used for external validation were not part of the model development, ensuring an unbiased evaluation of model performance. Validating a model via random samples from one-third of the data is a critical step for assessing robustness (Yu, et al., 2020). Our model validation tests revealed that NIRS can predict the FA composition of *Schizochytrium* in a reliable and accurate manner, which is consistent with previous studies showing that NIRS can be used to predict the FA composition of fish oil (Karunathilaka et al., 2019), pig fat (González-Martín et al., 2021), and milk-thistle whole seeds (Kolácková et al., 2015). In particular, our study showed that NIRS could accurately predict FA composition and notably, enhance detection efficiency, offering a time-efficient alternative to GC detection.

While 9.58 h was needed for GC analysis of a single sample, NIRS analysis was completed in 2 minutes (Table S1). NIRS proved effective, but Raman spectroscopy might also serve as an alternative for this application. Raman spectroscopy provides molecular vibration information, enabling rapid identification and quantification of metabolic products. Previous studies have demonstrated its potential in monitoring fermentation processes (Wang et al., 2014), quantifying lipids in microalgae with high accuracy compared to GC measurements (Lee et al., 2013), and predicting the FA composition of vegetable oils (Dong et al., 2013). While both NIRS and Raman spectroscopy are effective for rapid FA detection, our study focused on the application of NIRS. However, the throughput of the NIRS apparatus is limited by its reliance on manual sample changeovers. Thus, automated-sample changeover capabilities should be developed to further improve detection efficiency. Despite the limitations imposed by manual sample handling, NIRS significantly enhances detection efficiency and reduces costs, making it a valuable tool for analyzing and predicting the composition of fatty acids.

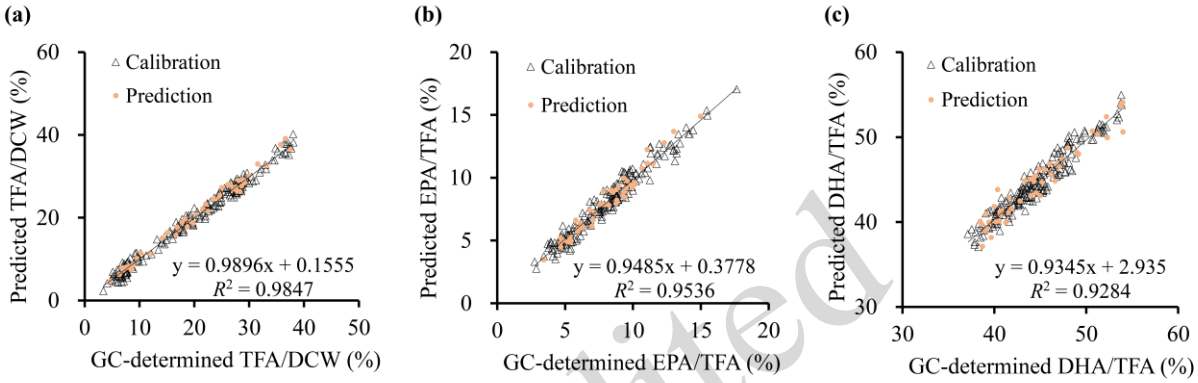

Fig. 3 Near-infrared spectroscopy (NIRS) prediction models for (a) TFA/DCW, (b) EPA/TFA, and (c) DHA/TFA. The black triangles represent the calibration model, the yellow circles represent the test data. The data were collected from three independent experiments.

3.3 Identifying mutants with high FA and EPA production

After GLPP mutagenesis, we selected more than 3000 mutants, cultured them in 48-well plates and then analyzed them with the NIRS models developed earlier. The predicted EPA/TFA and TFA/DCW values of the mutants are shown in Fig. 4a. The EPA/TFA ratio in 1469 mutants ranged from 2% to 21% with more than 53% of the mutants presenting higher levels of EPA/TFA than the WT strain, indicating that GLPP induces beneficial genetic mutations with good efficacy. Similarly, the TFA/DCW ranged from 3.4% to 63.3%, and more than 30% of the mutants presented greater TFA/DCW than the WT strain.

We calculated the EPA titer, which indicates the efficiency of EPA production by multiplying EPA/TFA, TFA/DCW, and DCW. As shown in Fig. 4b, the highest EPA titer achieved in a mutant M108 was 1.65 g/L, which was 3.24-fold greater than that of the WT strain. Concurrently, the EPA/TFA and TFA/DCW ratios were 8.67% and 50%, respectively. Another mutant exhibited a similar EPA titer of 1.47 g/L, but with markedly different EPA/TFA and TFA/DCW ratios (15.69% for EPA/TFA and 16.8% for TFA/DCW). These results indicated that the mutants could be divided into two distinct groups: those with higher TFA/DCW values and lower EPA/TFA values, and those with lower TFA/DCW values and higher EPA/TFA values. In a study carried out by Ou et al., the optimal mutant obtained from ARTP showed an EPA/TFA ratio of 5.86% and a TFA/DCW ratio of 59.2% (Ou, et al., 2023). Compared to ARTP, the use of GLPP led to a more significant variation in EPA/TFA. This difference may be attributable to the distinct mechanisms of the two types of mutagenesis. Although GLPP achievse a lethality rate of 93.5% in 15 min while ARTP reaches the same level in less than 1 min (Ou, et al., 2023; Wei, et al., 2023), GLPP can generate mutants with more diverse fatty-acid compositions; therefore, GLPP

effectively increases genetic diversity. On the basis of these results, GLPP mutagenesis can seems to be a valuable tool for enhancing the genetic diversity of microorganisms, potentially leading to the generation and isolation of mutants with new desirable properties.

We further evaluated the 48 mutants whose EPA/TFA ratios exceeded 15% via shake-flask fermentation. Among these 48 mutants, only six maintained the same EPA/TFA levels as the initially obtained mutants (Fig. 4c), and some mutants even presented lower EPA/TFA ratios (4.23%) than the WT strain. Therefore, most of the mutants were not stable. One explanation for this observation is that the DNA damage caused by the mutation triggered a DNA repair response, leading to elimination of the mutation and restoration of WT genetic sequences (Rosenberg, 2013; Chatterjee and Walker, 2017). This observation suggests that achieving stable and consistently high levels of EPA production could be a challenge, even though initial efforts to increase EPA/TFA through mutagenesis have shown promise. Nonetheless, we successfully identified three mutants that presented persistently high levels of EPA/TFA.

Stability tests are crucial for ensuring that genetic mutations are maintained under normal production conditions. No significant differences (P>0.05) in the EPA/TFA (Fig. 4d) or TFA/DCW (Fig. 4e) ratios were found across eight passages in three mutant strains: M7-25, 7-36, and 8-20. The average EPA/TFA ratios in these strains over eight passages were 14.83%, 13.65%, and 13.89%, respectively, and the TFA/DCW ratios were 26.17%, 26.24%, and 26.48%, respectively. These results suggest that the three mutants maintained stably across eight passages, indicating consistent genetic expression and metabolic performance. As shown in Fig. 4f, the EPA/TFA ratios of mutants M7-25, 7-36, and 8-20 were 2.42-, 2.08-, and 1.87-fold greater than those of the WT strain, respectively (P<0.05). Considering the degree of unsaturation, DHA and DPA were the most abundant unsaturated fatty acids, whereas C16:0 was the main saturated fatty acid. M7-25 was selected for further analysis by its high EPA/TFA (15.65%) and ARA/TFA (4.8%) ratios, as compared to other EPA-producing strains (Ou, et al., 2023).

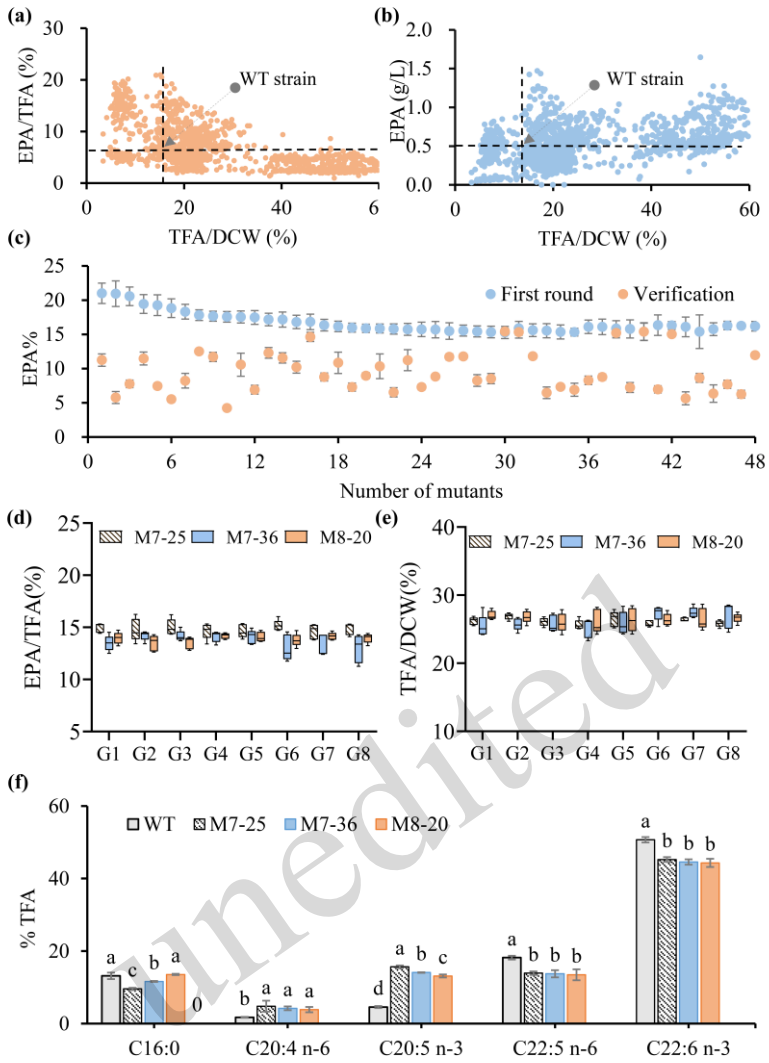

Fig. 4 High-throughput screening of *Schizochytrium* sp. mutants with highly efficient EPA production. (a) EPA titer and TFA/DCW of all the mutants cultured in 48-deep-well plates; (b) EPA/TFA and TFA/DCW of all the mutants cultured in 48-deep-well plates by near-infrared spectroscopy (NIRS) prediction; (c) Verification of EPA/TFA levels in the mutants grown through shake-flask cultivation; Stability test of (d) EPA/TFA and (e) TFA/DCW of the mutants M7-25, 7-36, and 8-20 grown across 8 generations through shake flask cultivation; (f) Main fatty-acid composition of the WT strain and the mutants M7-25, 7-36, and 8-20. C16:0 palmitic acid, C20:5 n3 eicosapentaenoic acid, C22:5 n6 docosapentaenoic acid, C22:6 n3 docosahexaenoic acid. The figures display average results obtained from at least three independent experiments, with error bars representing the standard deviation. Different lowercase letters indicate significant differences of each group based on Duncan's test (P<0.05).

We also identified a strong positive linear correlation with R^2=0.860 between EPA and ARA (Fig. S2), which has not been previously reported. According to a study conducted by Yue et al., ARA, EPA, DHA and DPA share a pool of acetyl-CoA and malonyl-CoA as precursors (Yue, et al., 2019), which may explain the observed decreases in DHA/TFA and DPA/TFA with the increase in EPA/TFA. Although *Schizochytrium* sp. is known to synthesize DHA and n-6 DPA via the PKS pathway, the EPA synthesis pathway involved remains elusive (Du et al., 2021). Nonetheless, the M7-25 mutant, which can synthesize high levels of EPA and ARA, may serve as a valuable resource for elucidating the EPA synthesis pathway. In conclusion, we identified a mutant (M7-25) with higher EPA/TFA and TFA/DCW levels than those of the WT strain, making it a suitable

candidate for further optimization experiments.

3.4 Medium optimization to increase TFA and EPA production

Schizochytrium sp. are typically found in coastal waters; consequently, salinity is a critical factor for their fatty-acid synthesis (Sun et al., 2018a). We investigated the influence of different concentrations of artificial sea salt and natural sea salt (NSS) on EPA production. As shown in Fig. 5a, the EPA/TFA ratio increased from 9.60% to 13.76% as the artificial sea salt concentration increased from 15 to 25 g/L but decreased to 9.65% at 45 g/L concentration (P<0.05). Similarly, the TFA/DCW decreased from 24% to 13.6% (Fig. 5b). In the NSS group, the highest EPA/TFA ratio was 9.5% with an NSS concentration of 15 g/L, but decreased to 2.88% with an NSS concentration of 45 g/L (Fig. 5a). Although the EPA/TFA ratio was lower in the NSS group, the TFA and TFA/DCW ratios were significantly greater than those in the artificial sea salt group (P<0.05). The highest TFA concentration achieved in the NSS group was 15.29 g/L, which was 69.3% greater than the highest TFA concentration attained in the artificial sea salt group (Fig. 5b). Studies have indicated that moderate salinity stress can increase lipid accumulation in *Schizochytrium* sp. whereas extreme salinity may inhibit lipid production (Sun et al., 2018b; Chen et al., 2023). Therefore, identifying the most appropriate salinity is essential for industrial production of lipids from *Schizochytrium* sp. The highest EPA titers attained in the artificial and natural salt groups were 1.15 and 1.37 g/L, respectively; both had a salinity of 25 g/L, but the EPA titer significantly decreased when the salinity increased to 45 g/L (P<0.05) (Fig. 5a).

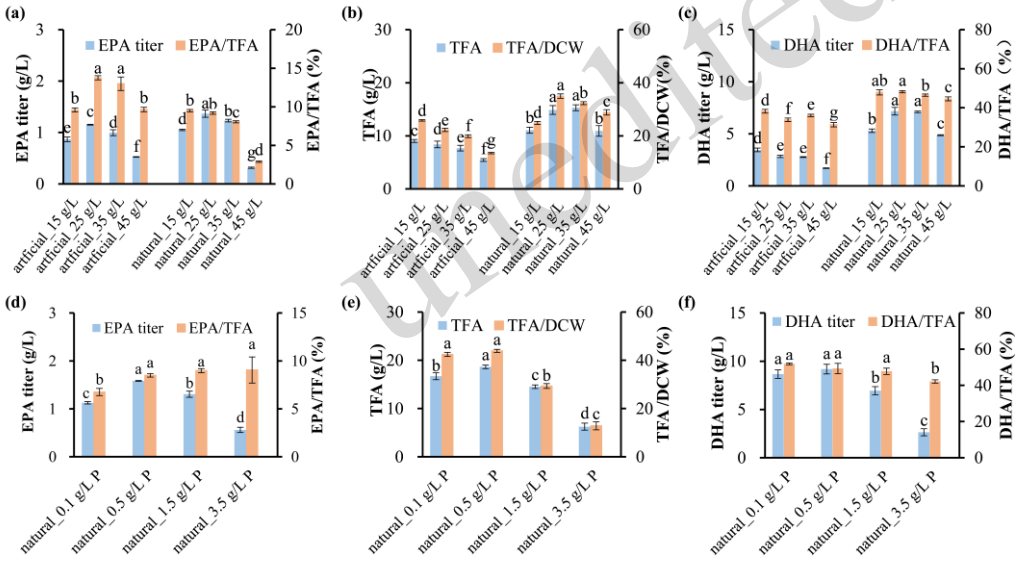

Fig. 5 Effects of different concentrations of artificial sea salt and natural sea salt (NSS) on (a) the EPA titer and EPA/TFA ratio; (b) TFA and TFA/DCW; and (c) the DHA titer and DHA/TFA in shake-flask fermentation of M7-25. Effect of different concentrations of phosphorus on (d) the EPA titer and EPA/TFA ratio; (e) TFA and TFA/DCW ratios; and (f) the DHA titer and DHA/TFA ratio in shake-flask fermentation of M7-25 with 25 g/L NSS. The figures show the average results obtained from three independent experiments, with error bars representing the standard deviation. Different lowercase letters indicate significant differences among groups according to Duncan's test (P<0.05)

Table 2 Extraction efficiency based on the fermentation of mutant strains

Batch	Strain	TFA (g/L)	TFA/DCW (%)	Theoretical TFA (g)	Extracted TFA (g)	Extraction efficiency
1#	M7-25	10.81	24.02%	97.3	25.8	26.52%

2#	M7-25	10.89	21.78%	98.0	27.0	27.55%
3#	M7-25	11.66	25.91%	186.6	42.0	22.51%
4#	M108	28.6	52.00%	257.4	221.0	85.86%

TFA: Total Fatty Acid, DCW: Dry Cell Weight

Considering the importance of lipid-extraction efficiency for algae-oil production, we applied two mutant strains (M7-25 and M108) in 7-L scale fermentation to obtain substantial biomass. M7-25 exhibits lower TFA/DCW but a higher EPA/TFA ratio, while M108, a mutant derived from GLPP mutagenesis, has opposite results (Fig. S3). Lipids were extracted after fermentation and the oil is shown in Fig. S4. As shown in Table 2, batch #2, with the lowest TFA/DCW ratio (21.78%), presented the lowest TFA extraction yield of 20.41%. In contrast, batch #4, with the highest TFA/DCW level (52.00%), demonstrated a markedly greater extraction TFA yield of 85.86%. This suggested that the TFA/DCW ratio is associated with TFA extraction efficiency. One possible explanation is that in low-lipid cells, lipids are more tightly bound within cell structures rather than being freely dispersed, making them less accessible to solvents. Additionally, higher proportions of non-lipid materials can hinder solvent penetration and lipid solubilization. Therefore, a higher TFA/DCW ratio enhances solvent access to lipids, resulting in increased extraction efficiency and yield. According to the study done by Derwenskus et al., the most expensive stage of the production of EPA from *Phaeodactylum tricornutum* is the extraction and purification process (Derwenskus et al., 2020). Therefore, culture with natural sea salt is more advantageous than with artificial sea salt. Chen et al. also demonstrated that NSS is suitable for producing oil from *Schizochytrium* sp (Chen, et al., 2023). Fig. 5c shows that both the DHA/TFA ratio and DHA titer were significantly greater in the NSS group than in the artificial sea salt group (P<0.05). This result further verified the idea that NSS is more suitable for promoting fatty-acid production from *Schizochytrium* sp.

Phosphorus is also essential for algae because it plays a crucial role in synthesizing phospholipids and triacylglycerols (Ren et al., 2013). As shown in Fig. 5d, increasing the KH_2PO_4 concentration from 0.1 to 1.5 g/L led to an increase of 30.8% in the EPA/TFA ratio (P<0.05). The highest EPA titer of 1.70 g/L was attained at 0.5 g/L KH_2PO_4. Fig. 5e shows that increasing the KH_2PO_4 concentration from 0.5 to 1.5 g/L resulted in a notable decrease in TFA/DCW and TFA (to 29.35% and 14.52 g/L, respectively), which further decreased to 12.83% and 6.25 g/L, respectively, as the KH_2PO_4 concentration increased to 3.5 g/L (P<0.05). Ren et al. reported that KH_2PO_4 concentrations between 0.1 and 0.5 g/L significantly increased TFA production, whereas higher concentrations decreased TFA production and the TFA/DCW ratio in *Schizochytrium* sp (Ren, et al., 2013). These findings suggest that KH_2PO_4 profoundly influences TFA synthesis in *Schizochytrium* sp. Fig. 5f shows that the DHA titer followed the same trend as that of TFA production; the DHA/TFA ratio significantly decreased at 3.5 g/L KH_2PO_4 (P<0.05). Therefore, 0.5 g/L KH_2PO_4 was optimal for both the EPA and DHA concentrations in NSS. In summary, we found that 25-35 g/L NSS and appropriate phosphate limitation are important for EPA and TFA production.

3.5 Fed-batch fermentation

The potential of mutant strain 7-25 for EPA production was validated in 7 L fermenters. Fig. 6a shows that the DCW of M7-25 did not significantly differ from that of the WT strain before 96 h. However, the amount of TFA produced by M7-25 reached a maximum of 17.01 g/L at 72 h, which was 35.8% greater than the maximum amount produced by the WT strain. This increase was mainly attributable to the higher TFA/DCW ratio in M7-25 than in the WT. Feeding with ammonia water (M7-25/NH_3 group) led to a notable improvement in both DCW and TFA production. The DCW in the M7-25/NH_3 group reached 63.0 g/L, which was 53.7% greater than that in the WT group (P<0.0001). The amount of TFA in the M7-25/NH_3 group increased to 23.19 g/L, representing a 53.4% increase compared with that in the WT group and an 81.6% increase compared with that in the M7-25 group at 96 h. The results shown in Fig. S5 demonstrate that the combination of $(NH_4)_2SO_4$ and NaOH

also supported cell growth and TFA production. In contrast, using a combination of NaOH and citrate acid to adjust pH resulted in lower DCW and TFA, suggesting that the absence of NH_4^+ limits both cell growth and lipid synthesis. The notable increase in TFA and DCW with the addition of ammonia indicates that nitrogen availability plays a crucial role in promoting cell growth and lipid synthesis. This finding aligns with those of a study by Yin et al., which showed that ammonia significantly promotes biomass and lipid accumulation in *Schizochytrium* sp. (Yin et al., 2019).

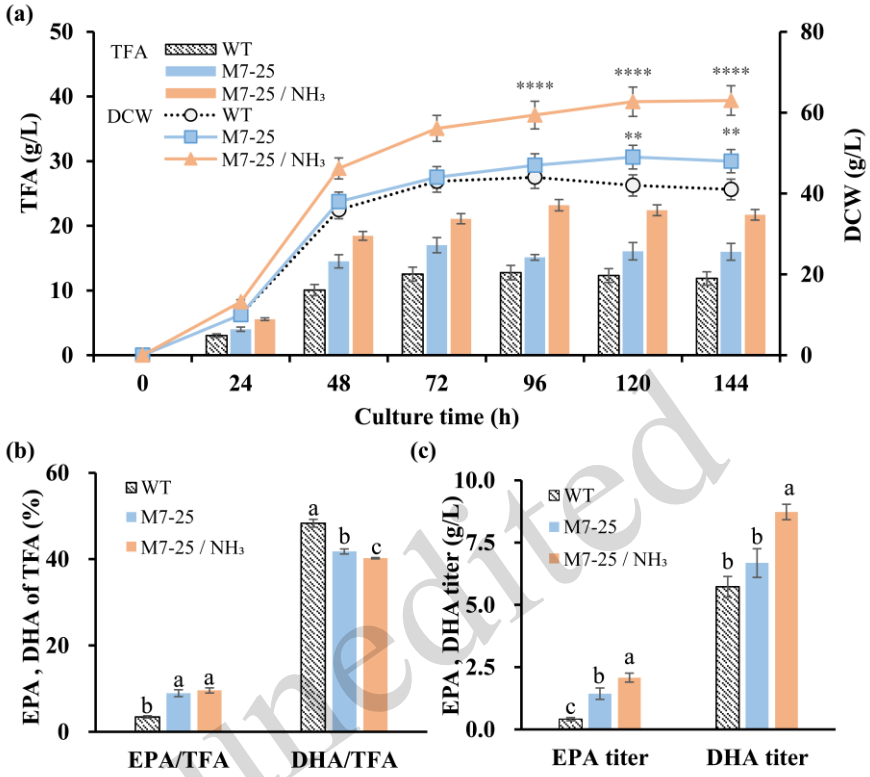

Fig. 6 Fed-batch fermentation of *Schizochytrium* sp. conducted in 7-L fermenters with different strains and fermentation strategies: WT (glucose feeding); M7-25 (glucose feeding); and M7-25/NH_3 (glucose and $NH_3 \cdot H_2O$ feeding). (a) Time courses of dry cell weight (DCW) and total fatty acid (TFA) in fed-batch culture; Significant differences among groups are indicated by asterisks (*P<0.05, **P<0.01, ***P<0.001, ****P<0.0001). (b) The ratios of EPA to TFA (EPA/TFA) and DHA to TFA (DHA/TFA) in *Schizochytrium* sp. at 144 h in fed-batch culture. (c) EPA and DHA titers in *Schizochytrium* sp. at 144 h in fed-batch culture. A 600 g/L glucose solution was added to the fermentation broth as needed to maintain a glucose concentration between 10 and 20 g/L. The air flow rate and agitation speed were adjusted to maintain dissolved oxygen levels above 20% during the initial 0–48 h and at 10% for the remaining 48–144 h. The figures show the average results obtained from at least three independent experiments, with error bars indicating the standard deviation. Different lower-case letters indicate significant differences among groups according to Duncan's test (P<0.05).

Fig. 6b shows that the EPA/TFA ratio in the M7-25/NH3 group reached 9.58%, which was 1.77-fold greater than the ratio in the WT group at the end of fermentation (P<0.05). Notably, a comparison between the M7-25 and M7-25/NH3 groups revealed that the EPA/TFA ratios were not significantly different, suggesting that ammonia supplementation had no effect on the EPA/TFA ratio (p>0.05). Additionally, the DHA/TFA level in the M7-25/NH3 group was comparable to that in the M7-25 group and 16.79% lower than that in the WT group. The noticeable reduction in the DHA/TFA level compared to that in the WT group highlights the effects of the induced mutations on fatty-acid synthesis in *Schizochytrium* sp. Finally, the EPA titer in the M7-25/NH3 group reached 2.08 g/L, which was 4.05-fold greater than that in the WT group (P<0.05). This is the greatest increase among the strains of *Schizochytrium* sp obtained by mutagenesis technology (Table 3). The DHA concentration

also increased by 52.4%, from 5.7 g/L to 8.7 g/L (Fig. 6c), indicating that ammonia supplementation with the M7-25 mutant substantially increased production of EPA and DHA. However, despite an impressive omega-3 production of 10.78 g/L, there remains a substantial gap compared to the industrial DHA production of 46.4 g/L (Chen et al., 2023), which poses a major bottleneck for industrialization. In addition to this, research on oil separation and purification processes is still needed to finalize the product. We speculate that the EPA production of M7-25 could be further improved by continued GLPP mutagenesis and fermentation optimization to facilitate large-scale industrial production of EPA in *Schizochytrium* sp. Furthermore, the combined GLPP and NIRS platform is not limited to optimizing EPA production in *Schizochytrium* sp.; it can also be applied to improve the efficiency of other microbial products. GLPP induces mutations throughout the genome, creating a diverse pool of mutants with potentially beneficial traits, while NIRS provides a non-destructive and rapid method to quantify desired products, enabling swift identification of high-performing strains. Therefore, when strains, whether genetically modified or not, reach the limits of their production capacity, this methodology offers an alternative route to discover unforeseen enhancements in production.

Table 3 The ability of *Schizochytrium* to produce EPA

Strain	Strategy	EPA/TFA (%)	EPA titer (mg/L)	Ref
Schizochytrium ATCC 20888	ARTP	3.47	480	(Zeng, et al., 2021)
Schizochytrium ATCC 20888	ARTP	5.87	1860	(Ou, et al., 2023)
Schizochytrium sp. *CABIO-A-2-IV*	GLPP	9.58	2080	This study

ARTP: Atmospheric and room-temperature plasma mutagenesis
GLPP: Gas-liquid-phase plasma mutagenesis
TFA: Total Fatty Acid
EPA: Eicosapentaenoic Acid

4 Conclusions

In conclusion, we developed an innovative strategy to increase EPA production in *Schizochytrium* sp. involving GLPP mutagenesis followed by NIRS screening, which enables the identification of high-yield strains from a 1469 mutant library in just one week. This method is much more efficient than traditional mutagenesis strategies. Compared with the WT strain, the M7-25 mutant presented a 1.77-fold increase in the EPA/TFA ratio and a 4.05-fold increase in the EPA titer. This is the greatest increase among the strains of *Schizochytrium* sp obtained by mutagenesis technology. This study lays the foundation for future strain mutagenesis and fermentation optimization for industrial-scale production of EPA as well as other omega-3 products from *Schizochytrium* strains.

Date availability statement

All data about this study are present in the article and supplementary data.

Acknowledgments

This work was supported by the National Key Research and Development Program of China (Grant No. 2021YFC2100800).

Author contributions

CY and JZ contributed equally to this paper. CY designed the research and finished writing the manuscript. JZ reviewed and revised the manuscript. CY, JZ, SZ, WZ and MS performed the experiments. SL and XL supported the work. JW and MW supervised the study. XC and JY conceptualized and supervised the study.

Compliance with ethics guidelines

The authors declare that they have no conflicts of interest.

References

Auchterlonie NA, Bescoby GH, 2021. Chapter 4 - global market for the long-chain omega-3 fatty acids epa and dha and their regulation. In: García-Moreno, P.J., Jacobsen, C., Moltke Sørensen, A.-D., et al. Eds.), Omega-3 delivery systems. Academic Press, p.79-106.

Bazinet RP, Metherel AH, Chen CT, et al., 2020. Brain eicosapentaenoic acid metabolism as a lead for novel therapeu tics in major depression. *Brain, Behav, Immun*, 85:21-28. https://doi.org/10.1016/j.bbi.2019.07.001

Bhatt DL, Steg PG, Miller M, et al., 2019. Effects of icosapent ethyl on total ischemic events: From reduce-it. *J Am Coll Cardiol*, 73(22):2791-2802. https://doi.org/10.1016/j.jacc.2019.02.032

Calder PC, 2013. N-3 fatty acids, inflammation and immunity: New mechanisms to explain old actions. *Proc Nutr Soc*, 72(3):326-336. https://doi.org/10.1017/S0029665113001031

Chatterjee N, Walker GC, 2017. Mechanisms of DNA damage, repair, and mutagenesis. *Environ Mol Mutagen*, 58(5):235-263. https://doi.org/10.1002/em.22087

Chen Z-L, Yang L-H, He S-J, et al., 2023. Development of a green fermentation strategy with resource cycle for the docosahexaenoic acid production by schizochytrium sp. *Bioresour Technol*, 385:129434. https://doi.org/10.1016/j.biortech.2023.129434

Derwenskus F, Weickert S, Lewandowski I, et al., 2020. Economic evaluation of up- and downstream scenarios for the co-production of fucoxanthin and eicosapentaenoic acid with p. Tricornutum using flat-panel airlift photobioreactors with artificial light. *Algal Res*, 51:102078. https://doi.org/10.1016/j.algal.2020.102078

Doaei S, Gholami S, Rastgoo S, et al., 2021. The effect of omega-3 fatty acid supplementation on clinical and biochemical parameters of critically ill patients with covid-19: A randomized clinical trial. *J Transl Med*, 19(1):128. https://doi.org/10.1186/s12967-021-02795-5

Dong W, Zhang Y, Zhang B, et al., 2013. Rapid prediction of fatty acid composition of vegetable oil by raman spectroscopy coupled with least squares support vector machines. *Journal of Raman Spectroscopy*, 44(12):1739-1745. https://doi.org/https://doi.org/10.1002/jrs.4386

Du F, Wang Y-Z, Xu Y-S, et al., 2021. Biotechnological production of lipid and terpenoid from thraustochytrids. *Biotechnol Adv*, 48:107725. https://doi.org/10.1016/j.biotechadv.2021.107725

Golay P-A, Moulin J, 2016. Determination of labeled fatty acids content in milk products, infant formula, and adult/pediatric nutritional formula by capillary gas chromatography: Collaborative study, final action 2012.13. *J AOAC INT*, 99(1):210-222.

González-Martín MI, Escuredo O, Hernández-Jiménez M, et al., 2021. Prediction of stable isotopes and fatty acids in subcutaneous fat of iberian pigs by means of nir: A comparison between benchtop and portable systems. *Talanta*, 224:9. https://doi.org/10.1016/j.talanta.2020.121817

Gupta A, Wilkens S, Adcock JL, et al., 2013. Pollen baiting facilitates the isolation of marine thraustochytrids with potential in omega-3 and biodiesel production. *J Ind Microbiol Biotechnol*, 40(11):1231-1240. https://doi.org/10.1007/s10295-013-1324-0

Hamilton HA, Newton R, Auchterlonie NA, et al., 2020. Systems approach to quantify the global omega-3 fatty acid cycle. *Nat Food*, 1(1):59-62. https://doi.org/10.1038/s43016-019-0006-0

Jia Y-L, Geng S-S, Du F, et al., 2022. Progress of metabolic engineering for the production of eicosapentaenoic acid. *Critical Reviews in Biotechnology*, 42(6):838-855. https://doi.org/10.1080/07388551.2021.1971621

Jiang Y, Fan K-W, Tsz-Yeung Wong R, et al., 2004. Fatty acid composition and squalene content of the marine micro alga schizochytrium mangrovei. *J Agr Food Chem*, 52(5):1196-1200. https://doi.org/10.1021/jf035004c

Karunathilaka SR, Choi SH, Mossoba MM, et al., 2019. Rapid classification and quantification of marine oil omega-3 supplements using atr-ftir, ft-nir and chemometrics. *J Food Compos Anal*, 77:9-19. https://doi.org/10.1016/j.jfca.2018.12.009

Khan SU, Lone AN, Khan MS, et al., 2021. Effect of omega-3 fatty acids on cardiovascular outcomes: A systematic review and meta-analysis. *EClinicalMedicine*, 38:100997. https://doi.org/10.1016/j.eclinm.2021.100997

Kolácková P, Ruzicková G, Gregor T, et al., 2015. Quick method (ft-nir) for the determination of oil and major fatty acids content in whole achenes of milk thistle (silybum marianum (l.) gaertn.). *J Sci Food Agric*, 95(11):2264-2270. https://doi.org/10.1002/jsfa.6945

Kosmopoulos A, Bhatt DL, Meglis G, et al., 2021. A randomized trial of icosapent ethyl in ambulatory patients with covid-19.

iScience, 24(9):103040. https://doi.org/10.1016/j.isci.2021.103040

Lamon-Fava S, So J, Mischoulon D, et al., 2021. Dose- and time-dependent increase in circulating anti-inflammatory and pro-resolving lipid mediators following eicosapentaenoic acid supplementation in patients with major depressive disorder and chronic inflammation. *Prostaglandins Leukot Essent Fatty Acids*, 164:102219. https://doi.org/10.1016/j.plefa.2020.102219

Lee T-H, Chang J-S, Wang H-Y, 2013. Rapid and in vivo quantification of cellular lipids in chlorella vulgaris using n ear-infrared raman spectrometry. *Analytical Chemistry*, 85(4):2155-2160. https://doi.org/10.1021/ac3028118

Ling X, Guo J, Liu X, et al., 2015. Impact of carbon and nitrogen feeding strategy on high production of biomass and docosahexaenoic acid (dha) by schizochytrium sp. Lu310. *Bioresour Technol*, 184:139-147. https://doi.org/10.1016/j.biortech.2014.09.130

Liu L, Bai MH, Zhang S, et al., 2021a. Artp mutagenesis of schizochytrium sp. Pku#mn4 and clethodim-based mutant screening for enhanced docosahexaenoic acid accumulation. *Mar Drugs*, 19(10):564. https://doi.org/10.3390/md19100564

Liu Y, Tian Y, Cai W, et al., 2021b. Dha/epa-enriched phosphatidylcholine suppresses tumor growth and metastasis via activating peroxisome proliferator-activated receptor γ in lewis lung cancer mice. *J Agr Food Chem*, 69(2):676-685. https://doi.org/10.1021/acs.jafc.0c06890

Morabit Y, Hasan MI, Whalley RD, et al., 2021. A review of the gas and liquid phase interactions in low-temperature plasma jets used for biomedical applications. *The European Physical Journal D*, 75(1):32. https://doi.org/10.1140/epjd/s10053-020-00004-4

Ou Y, Li Y, Feng S, et al., 2023. Transcriptome analysis reveals an eicosapentaenoic acid accumulation mechanism in a schizochytrium sp. Mutant. *Microbiol Spectr*, 11(3):e0013023. https://doi.org/10.1128/spectrum.00130-23

Peng Z, Zhang C, Yan L, et al., 2020. Epa is more effective than dha to improve depression-like behavior, glia cell dysfunction and hippcampal apoptosis signaling in a chronic stress-induced rat model of depression. *Int J Mol Sci*, 21(5):1769. https://doi.org/10.3390/ijms21051769

Preston Mason R, 2019. New insights into mechanisms of action for omega-3 fatty acids in atherothrombotic cardiovascular disease. *Curr Atheroscler Rep*, 21(1):2. https://doi.org/10.1007/s11883-019-0762-1

Ratledge C, Hopkins S, 2006. 23 - applications and safety of microbial oils in food. In: Gunstone, F.D. (Ed. Modifying lipids for use in food. Woodhead Publishing, p.567-586.

Reis MG, Agnew M, Jacob N, et al., 2022. Comparative evaluation of miniaturized and conventional nir spectrophotometer for estimation of fatty acids in cheeses. *Spectrochim Acta, Part A*, 279:121433. https://doi.org/10.1016/j.saa.2022.121433

Ren L-J, Feng Y, Li J, et al., 2013. Impact of phosphate concentration on docosahexaenoic acid production and related enzyme activities in fermentation of schizochytrium sp. *Bioprocess Biosyst Eng*, 36(9):1177-1183. https://doi.org/10.1007/s00449-012-0844-8

Rosenberg SM, 2013. Reverse mutation. In: Maloy, S., Hughes, K. Eds.), Brenner's encyclopedia of genetics. Academic Press, San Diego, California, p.220-221.

Shen J, Zhang H, Xu Z, et al., 2019. Preferential production of reactive species and bactericidal efficacy of gas-liquid plasma discharge. *Chem Eng J*, 362:402-412. https://doi.org/10.1016/j.cej.2019.01.018

Shene C, Paredes P, Vergara D, et al., 2020. Antarctic thraustochytrids: Producers of long-chain omega-3 polyunsaturated fatty acids. *MicrobiologyOpen*, 9(1):e00950. https://doi.org/10.1002/mbo3.950

Sun X-M, Ren L-J, Bi Z-Q, et al., 2018a. Adaptive evolution of microalgae schizochytrium sp. Under high salinity stress to alleviate oxidative damage and improve lipid biosynthesis. *Bioresour Technol*, 267:438-444. https://doi.org/10.1016/j.biortech.2018.07.079

Sun X-M, Ren L-J, Bi Z-Q, et al., 2018b. Development of a cooperative two-factor adaptive-evolution method to enhance lipid production and prevent lipid peroxidation in schizochytrium sp. *Biotechnol Biofuels*, 11(1):65. https://doi.org/10.1186/s13068-018-1065-4

Tsegay G, Ammare Y, Mesfin S, 2023. Development of non-destructive nirs models to predict oil and major fatty acid contents of ethiopian sesame. *J Food Compos Anal*, 115 https://doi.org/10.1016/j.jfca.2022.104908

Wang Q, Li Z, Ma Z, et al., 2014. Real time monitoring of multiple components in wine fermentation using an on-li ne auto-calibration raman spectroscopy. *Sensors and Actuators B: Chemical*, 202:426-432. https://doi.org/https://doi.org/10.1016/j.snb.2014.05.109

Wang S, Wan W, Wang Z, et al., 2021. A two-stage adaptive laboratory evolution strategy to enhance docosahexaenoi c acid synthesis in oleaginous thraustochytrid. *Front Nutr*, 8, :795491. https://doi.org/10.3389/fnut.2021.795491

Wei X, Wang Y, Liu X, et al., 2023. Metabolic analysis of schizochytrium sp. Mutants with high epa content achieved with artp mutagenesis screening. *Bioprocess Biosyst Eng*, 46(6):893-901. https://doi.org/10.1007/s00449-023-02874-5

Xiao B, Li Y, Lin Y, et al., 2022. Eicosapentaenoic acid (epa) exhibits antioxidant activity via mitochondrial modulation. *Food Chem*, 373:131389. https://doi.org/10.1016/j.foodchem.2021.131389

Yin F-W, Zhang Y-T, Jiang J-Y, et al., 2019. Efficient docosahexaenoic acid production by schizochytrium sp. Via a two-phase ph control strategy using ammonia and citric acid as ph regulators. *Process Biochem*, 77:1-7. https://doi.org/10.1016/j.procbio.2018.11.013

Yin H, Liu Y, Yue H, et al., 2022. Dha- and epa-enriched phosphatidylcholine suppress human lung carcinoma 95d cells metastasis via activating the peroxisome proliferator-activated receptor γ. *Nutrients*, 14(21):4675. https://doi.org/10.3390/nu14214675

Yu H, Liu H, Wang Q, et al., 2020. Evaluation of portable and benchtop nir for classification of high oleic acid peanuts and fatty acid quantitation. *LWT*, 128 https://doi.org/10.1016/j.lwt.2020.109398

Yue X-H, Chen W-C, Wang Z-M, et al., 2019. Lipid distribution pattern and transcriptomic insights revealed the potential mechanism of docosahexaenoic acid traffics in schizochytrium sp. A-2. *J Agr Food Chem*, 67(34):9683-9693. https://doi.org/10.1021/acs.jafc.9b03536

Zeng L, Bi YQ, Guo PF, et al., 2021. Metabolic analysis of schizochytrium mutants with high dha content achieved with artp mutagenesis combined with iodoacetic acid and dehydroepiandrosterone screening. *Bioprocess Biosyst Eng*, 9:738052. https://doi.org/10.3389/fbioe.2021.738052

Zeng W, Guo L, Xu S, et al., 2020. High-throughput screening technology in industrial biotechnology. *Trends Biotechnol*, 38(8):888-906. https://doi.org/10.1016/j.tibtech.2020.01.001

Supplementary information:

Near-infrared spectroscopy (NIRS) of *Schizochytrium* sp. cultivation broth from different mutants (Fig. S1); correlation between EPA/TFAs and ARA/TFAs of all the mutants cultured in a 48-deep-well plate (Fig. S2); Stability test of (a) EPA/TFA and (b) TFA/DCW of the M108 mutants grown across 5 generations through shake-flask cultivation (Fig. S3); EPA oil refined from four fermentations using different mutants (Fig. S4); Effects of different concentrations of acid-base regulators on (a) DCW; (b) TFA; (c) EPA/TFA; and (d) DHA/TFA in 7-L fermentation of M7-25 (Fig. S5); time cost of fatty-acid composition analysis via near infrared spectroscopy (NIRS) compared with gas chromatography (GC) analysis (Table S1).